Central European Journal of Energetic Materials
ISSN 1733-7178; e-ISSN 2353-1843

Cent. Eur. J. Energ. Mater., 2016, *13*(3), 658-676; DOI: 10.22211/cejem/65004

Theoretical and Experimental Study on Detonation Wave Propagation in Cylindrical High Explosive Charges with a Wave-shaper

Jian PAN,[1] Xianfeng ZHANG,[1*] Yong HE,[1]
Qibin DENG,[1] Zhongwei GUAN [2]

[1] *School of Mechanical Engineering, Nanjing University of Science and Technology, Xiaolingwei 200, Nanjing 210094, China*
[2] *School of Engineering, University of Liverpool, Brownlow Street, Liverpool L69 3GQ, UK*
[*] *E-mail: lynx@mail.njust.edu.cn*

Abstract: The use of a cylindrical high-explosive charge with a wave-shaper is an efficient way to obtain an ultra-high pressure and a convergent detonation wave. An analysis of flow fields corresponding to the regular and Mach reflection of detonation waves in a cylindrical high-explosive charge with a wave-shaper is presented in this paper. The pressure, flow velocity and triple point growth angle of the Mach stem were calculated. The Mach stem height was also determined by using the modified Whitham method. The results show that the Mach stem height rises from zero at the critical angle of Mach reflection and changes to the Chapman-Jouguet detonation state with the propagation of the detonation waves. Shock indentation experiments were conducted, in which a wave-shaper was used in a cylindrical high-explosive charge to form Mach reflection detonation waves. The results showed that the discrepancy between the experimental results and the theoretical calculations was less than 15%, which proves the validity of the proposed theoretical model.

Keywords: high explosive, detonation wave, Mach reflection, wave-shaper, Whitham method

1 Introduction

In recent years, researchers have investigated various methods for obtaining ultra-high detonation pressures and for controlling the detonation wave shape in order to further increase the utilization factor of a high-explosive charge.

Annular (multipoint) initiation using a wave-shaper and double layer charges are the most commonly used techniques for obtaining an optimized detonation wave to efficiently accelerate a shaped charge penetrator. For double layer charges, due to the shock induced by initiation of the outer layer high-explosive charge, the detonation wave in the inner charge is delayed relative to that of the outer layer charge. Here, the detonation wave will satisfy a steady state condition and ultimately propagates with a constant shape. Using a cylindrical high-explosive charge with a wave-shaper is an efficient way of achieving convergent detonation wave propagation and of generating regular or Mach reflection at the axis of symmetry of the charge. Figure 1 shows a schematic of a cylindrical high-explosive charge with a wave-shaper. The charge is initiated at the center of one end, resulting in the propagation of an annular initial detonation wave due to the effect of the wave-shaper. Huygens' Principle [1] states that the annular initial detonation wave interacts at the axis of symmetry of the charge. Regular or Mach reflection then occurs during detonation wave propagation.

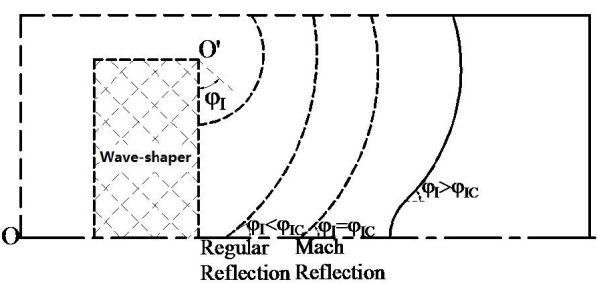

Figure 1. Configuration of a cylindrical high-explosive charge with a wave-shaper.

A cylindrical high-explosive charge with a wave-shaper is mainly used in shaped charges to increase the jet velocity of the shaped charge in high-explosive anti-tank warheads, or to improve the performance of Explosively Formed Projectiles [2, 3]. Researchers around the world have conducted extensive studies on detonation wave propagation and interaction with regular/Mach reflection. As early as the 1970s, Al'tshuler *et al*. [4] used a special experimental method to observe the detonation wave interaction of Composition B explosives. Their results showed that the maximum value of the detonation velocity resulting from overdriven detonation might be double the normal detonation velocity, and the pressure value exceeded 120 GPa. Dunne [5, 6] conducted theoretical and experimental studies on the Mach reflection of a detonation wave in condensed high-explosives to determine the critical angle for the Mach reflection and the

pressure in the centre of the Mach stem. Krishnan *et al*. [7] presented experimental results of Mach reflection in condensed high explosives viz., triple point growth angle, Mach-disc configuration and pressure. Trotsyuk *et al*. [8] investigated the effect of the existence of strong transverse waves on the Mach stem front and the steadiness of Mach reflection. Wang [9] calculated the Mach stem height in an unsteady Mach reflection by using a cylindrical convex surface. Based on the calculation of the Mach stem height in pseudo-steady Mach reflection, the locus of the triple point was obtained by integrating a suitable vector field. Hull [10, 11] determined the relationship between detonation velocity and local wave curvature for the Mach reflection of a spherical detonation wave. Mach stem formation was observed in the course of the calibration of convergent flow in Hull's detonation wave reflection experiments [10, 11]. Zhang *et al*. [12] used an analytical model and numerical simulations to investigate the regular and Mach reflection during the detonation wave propagation in double-layer cylindrical high-explosive charges. The pressure, flow velocity and specific volume were calculated and the Mach stem height was determined from mass conservation in the flow field.

Cao *et al*. [13] conducted an experimental study on the detonation wave propagation in cylindrical high-explosive charges with two-point initiation and presented indentation results on copper targets to verify the Mach reflection. Due to the density of the explosive being the same, by changing the diameter or length of the explosive charge, different indentation shapes can be obtained on the surface of the copper targets. Therefore, the propagation characteristics of the detonation wave and the Mach stem can be obtained. Fan *et al*. [14] presented the detonation wave interaction and propagation in a cylindrical high-explosive with a wave-shaper. The pressure and flow velocity at different positions of the wave front were determined based on experimental and theoretical approaches.

Theoretical, numerical and experimental studies available in the literature have mostly focused on critical reflection conditions as well as the increase in the pressure and velocity of the Mach reflection of detonation waves. To date, limited analytical work has been carried out to explore the details of Mach reflection, such as the pressure distribution and the Mach stem height for a cylindrical high-explosive charge. Analytical models and experimental studies have rarely been used to describe detonation wave propagation with Mach reflection in a cylindrical high-explosive charge with a wave-shaper.

An analytical model for detonation wave propagation in a cylindrical HE charge with a wave-shaper is presented in this paper. The pressure and triple point growth angle of the Mach stem in a cylindrical high-explosive charge with a wave-shaper have been determined using the three-shock theory and the

modified Whitham method. Flow fields associated with the regular and Mach reflection of detonation waves were analyzed. In addition, an analytical model for predicting the Mach stem height is proposed. To validate the analytical results, shock indentation experiments on a copper target were performed using 50 mm diameter cylindrical HE charges, with and without a wave-shaper.

2 Analytical Model in a Cylindrical High-Explosive with a Wave-shaper

2.1 Detonation wave propagation in a cylindrical high-explosive with a wave-shaper

Figure 2 shows sketches of detonation waves with regular reflection and Mach reflection, in which two equal intensity detonation waves colliding with each other are considered, corresponding to the oblique impact of a detonation onto a rigid surface [14]. When the incident angle φ_I is smaller than the critical angle φ_{IC}, the incident detonation front (I) intersects with the reflected shock (R) at point P, which is a point on the line of collision. In passing through this discontinuity, the flow becomes parallel to the collision line and is then deflected upwards again with an angle $\theta_2 = \theta_1$, as shown in Figure 2a. When the incident angle reaches the critical angle, the deflection angle θ_2 becomes smaller than θ_1. The flow mass will be accumulated, thereby forcing the collision point P to move to point Q, as shown in Figure 2b. The parameters in each region are defined according to the descriptions presented by Grasso and Paoli [15] and Chpoun *et al*. [16] on Mach reflection which induces detonation in a reactive flow.

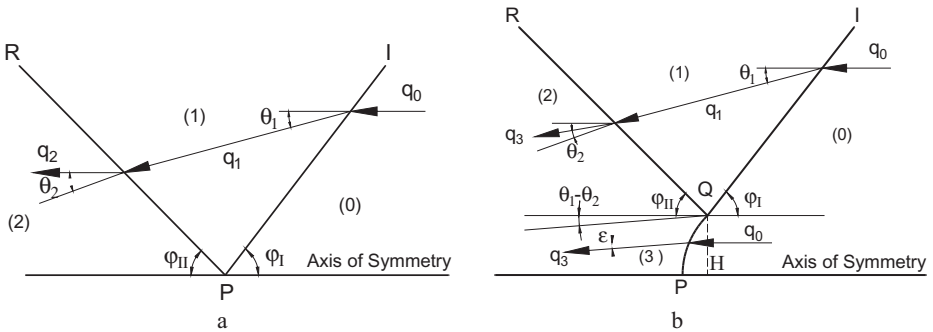

Figure 2. Flow setup used to describe: (a) regular reflection and (b) Mach reflection.

Assuming that the explosives react completely and satisfy the Chapman-

Jouguet detonation condition, the parameters of region (1) are obtained as a function of the initial density ρ_0, the polytrophic exponent γ, the incident angle, and the Chapman-Jouguet detonation parameters. According to the geometric relationship, the deflection angle θ_1 can be written as follows:

$$\tan\theta_1 = \frac{\tan\varphi_1}{\gamma\cdot\tan^2\varphi_1 + (\gamma+1)} \tag{1}$$

For the flow field from regions (0) to (1), the deflection angle θ_1 and the reflection angle $\varphi_I + \varepsilon$ satisfy the following relationship:

$$\tan\theta_1 = \frac{[M_1^2\cdot\sin^2(\varphi_{II}+\varepsilon)-1]\cdot\tan^{-1}(\varphi_{II}+\varepsilon)}{M_1^2\cdot[(\gamma+1)/2-\sin^2(\varphi_{II}+\varepsilon)]+1} \tag{2}$$

where M_1 is the Mach number of region (1), $M_1 = \sqrt{1+(\gamma+1)^2/(\gamma\tan\varphi_I)^2}$; $\varepsilon = \theta_1$ and $\varepsilon = (\theta_2 - \theta_1)$ are the regular and Mach reflections, respectively.

The deflection angle θ_1 and the reflection angle can be determined by using Equations 1 and 2. The parameters of three typical high-explosives are listed in Table 1. Figure 3 shows that the deflection angle θ_1 rises from zero to the maximum value corresponding to the incident angle, from zero to the critical reflection angle, and then declines to zero as the incident angle increases to $\pi/2$. Figure 4 shows that the deflection angle θ_2 reaches its maximum value at the critical angle, and then decreases to zero for RDX explosive. The critical angle is obtained, based on the condition that Equation 2 has no solution. The calculated values of the critical angle, listed in Table 1, concur reasonably well with the experimental results from the literature.

Table 1. Parameters of different high explosives [4, 7, 9]

High Explosive	ρ_0 [g·cm^{-3}]	D_{CJ} [ms^{-1}]	γ	φ_{IC}	
				Exp.	Cal.
RDX	1.80	8754	2.980	44.5°±2°	44.7°
TNT	1.63	6930	3.120	45.6°	44.12°
PBX9501	1.832	8802	2.097	56.0°	48.13°

Consistent with extensive theoretical and experimental research efforts [17, 20], the Mach stem is characterized as a curved shape, normal to the axis of symmetry at point P, and tangential to the detonation front at point Q. Thus, the difference value of the deflection angle is not a constant on the Mach stem from

point P to point Q, and the angle of the tangent line at the Mach stem to the axis of symmetry is variable. According to the conservation of mass and momentum, the parameters of the Mach stem can be defined as follows:

$$P_3 = \rho_0 \cdot \left(\frac{D_{CJ}}{\sin \varphi_I} \cdot \sin \beta \right)^2 \cdot \left(1 - \frac{\rho_0}{\rho_3} \right) \tag{3}$$

$$\rho_3 = \frac{\rho_0 \cdot \tan \beta}{\tan\left[\beta - (\theta_1 - \theta_2)\right]} \tag{4}$$

$$q_3 = \frac{\rho_0}{\rho_3} \cdot \frac{D_{CJ} \cdot \sin \beta}{\sin \varphi_I \cdot \sin\left[\beta - (\theta_1 - \theta_2)\right]} \tag{5}$$

where D_{CJ} is the Chapman-Jouguet detonation velocity, and P_3, ρ_3 and q_3 are the detonation pressure, density and velocity of the Mach reflection, respectively.

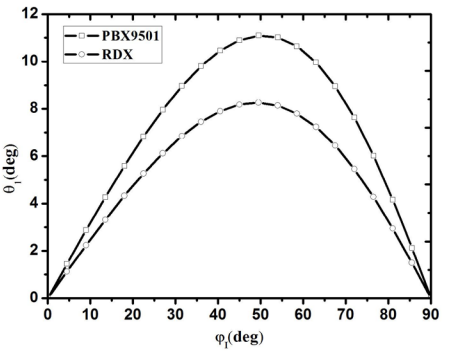

Figure 3. Calculated deflection angle θ_1.

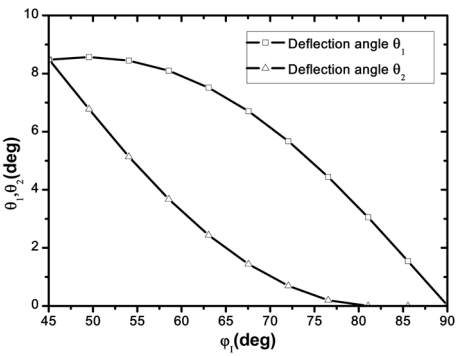

Figure 4. Calculated θ_1 and θ_2 for RDX.

According to Sternberg's definition [21], when Mach reflection occurs, a slip line appears inside the detonation products emanating from the triple point. This line is a streamline across, within which the pressure is continuous but the velocity and the density are not. Therefore, the pressure of the triple point Q, which is equal to that in regions (2) and (3), can be defined as follows:

$$\frac{P_Q}{P_1} = \frac{2\gamma}{\gamma+1} \cdot M_1^2 \cdot \sin^2(\varphi_{II} + \theta_1) - \frac{\gamma-1}{\gamma+1} \tag{6}$$

where $P_1 = \rho_0 \cdot D_I^2 / (\gamma + 1)$.

The pressure and the density at the collision point P are difficult to obtain from Equations 3 and 5. According to Sternberg's results [21], the Chapman-Jouguet detonation parameters for pentolite (TNT/PETN (50/50)) are $P_{CJ} = 24.52$ GPa, $D_{CJ} = 7655$ m/s and $\rho_{CJ} = 2.21$ g/cm^3. The pressure at the triple point Q and the collision point P for different incident angles are determined, as shown in Figure 5. The results show that the ratio of the pressure behind the reflected shock to the Chapman-Jouguet pressure during regular reflection is constant. As the incident angle increases, Mach reflection occurs at $\varphi_I = 45.6°$ and the pressure reaches its maximum at the collision and the triple point and then decreases as the incident angle increases. When the incident angle increases to approximately $\pi/2$, the pressure at the collision and at the triple point is equal to the Chapman-Jouguet pressure, indicating that the convergent detonation wave induced by the wave-shaper ultimately has a diverging spherical shape.

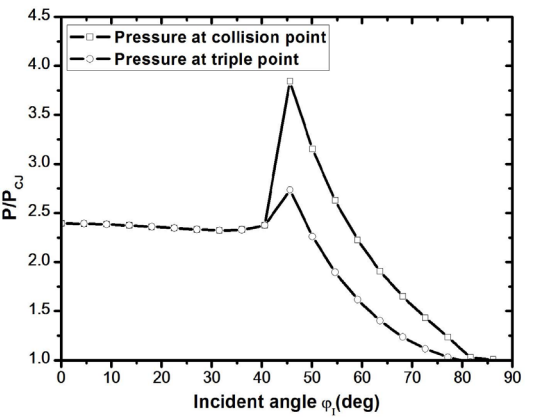

Figure 5. Calculated pressure versus incident angle at the triple and collision points.

2.2 Mach stem height model

In the current study, in consideration of the Whitham method [22, 23], the local Mach number is assumed to be a function of the ray tube area. According to the shock-shock of Whitham's geometrical shock dynamics, under a two-dimensional condition, the shock positions and rays form an orthogonal coordinate system, as shown in Figure 6. The differential relationship between the intensity of the detonation wave and the cross section of the flow is defined as follows:

$$-\frac{1}{A}\cdot\frac{dA}{dz}=\frac{1}{\gamma\cdot z}+\frac{1}{2z-1}+\frac{\gamma\cdot z+1}{\left\{\gamma\cdot z^{2}\cdot(2z-1)\cdot\left[(\gamma-1)\cdot z+1\right]\right\}^{1/2}} \tag{7}$$

where A is the cross-sectional area, $z = P_3 / P_{CJ}$ is the intensity of the detonation wave, in which P_3 and P_{CJ} are the pressures of the Mach reflection and the Chapman-Jouguet detonation, respectively.

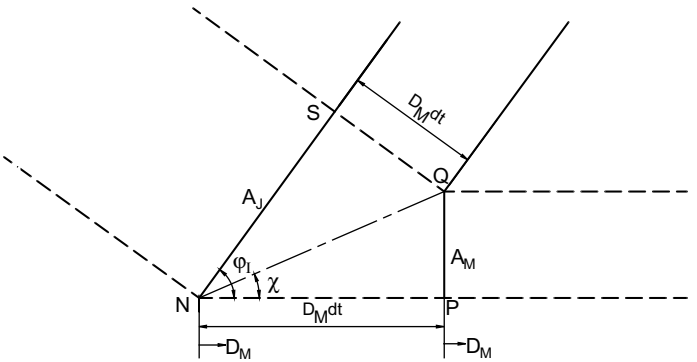

Figure 6. Shock-shock of Whitham's geometrical shock dynamics.

Assuming that Equation 7 satisfies the condition of the limited variation of cross-sectional area, $A(z)$ can be obtained by integrating Equation 7:

$$A\cdot f(z)=A_0\cdot f(z)=const \tag{8}$$

where

$$f(z)=z^{1/\gamma}\cdot(2z-1)^{1/2}\cdot B(z)\cdot C(z)$$

$$B(z)=\left\{\left[2(\gamma-1)\cdot(2z-1)\right]^{1/2}+2\left[(\gamma-1)\cdot z+1\right]^{1/2}\right\}^{\left[2\gamma/(\gamma-1)\right]^{1/2}}$$

$$C(z) = \exp\left\{\gamma^{-1/2} \cdot \sin^{-1}\left[\frac{(3-\gamma)\cdot z - 2}{(\gamma+1)\cdot z}\right]\right\}$$

Based on the above description, after a time increment, the detonation wave turns into the Mach wave, as shown in Figure 6. The relationship between the incident angle and the triple point growth angle is further defined as follows:

$$\tan\varphi_I = \left(\frac{D_{CJ}}{D_M} + \frac{A_M}{A_{CJ}}\right)\cdot\left\{\left[1-\left(\frac{D_{CJ}}{D_M}\right)^2\right]\cdot\left[1-\left(\frac{A_M}{A_{CJ}}\right)^2\right]\right\}^{-(1/2)} \tag{9}$$

$$\cos\chi / \sin(\varphi_I - \chi) = D_M / D_{CJ} \tag{10}$$

$$\sin\chi / \cos(\varphi_I - \chi) = A_M / A_{CJ} \tag{11}$$

where χ is the triple point growth angle of the Mach reflection, A_{CJ} and A_M are the cross-sections of NS and PQ.

The following relationship can be obtained from Equation 8:

$$A_M / A_{CJ} = f(1) / f(z) \tag{12}$$

According to the formula reported by Lambourn and Wright [24], the relationship between the detonation velocity of Mach reflection and the detonation velocity of Chapman-Jouguet is given by:

$$\frac{D_M}{D_{CJ}} = \frac{\mathrm{z}}{(2z-1)^{1/2}} \tag{13}$$

where D_M is the detonation velocity of Mach reflection and D_{CJ} is the detonation velocity of Chapman-Jouguet.

In the above calculation, when the rarefaction wave is disregarded, the calculation results will have large deviations. Therefore, $A(z)$ is modified [24] as follows:

$$A_{CJ} / A_M = (2\mathrm{z} - 1)^{1/2k(z)} \tag{14}$$

where $k(z)$ is generally considered as a constant. The values of the detonation velocity of Mach reflection, z, and the triple point growth angle of Mach reflection can be determined from Equations 9 to 14.

Table 2. Comparison of the results of the parameters of Mach reflection

The incident angle	Detonation velocity of Chapman-Jouguet [m/s]	$k(z)$	Experimental results [25]		Calculation results	
			Detonation velocity of Mach reflection [m/s]	The triple point growth angle of Mach reflection	Detonation velocity of Mach reflection [m/s]	The triple point growth angle of Mach reflection
46.5°	4140	0.27	5890	1.50°	5860	1.55°
48.5°	4200	0.29	5770	2.27°	5790	2.13°
49.5°	4480	0.30	6070	2.80°	6110	2.45°

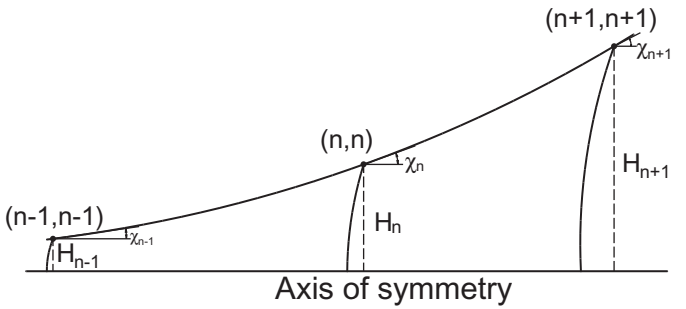

Figure 7. Variation of Mach reflection height at different grid points.

The results show that with the propagation of detonation waves, the triple point growth angle of a Mach reflection is not constant but varies with changes in the incident angle, $k(z)$ and the detonation velocity. With the use of experimental results from the literature [25], the parameters of the Mach reflection are listed in Table 2. The calculation results are consistent with the experimental results, indicating that the triple growth angle of Mach reflection can be determined by using the modified Whitham method [22, 23].

Given that the Chapman-Jouguet detonation velocity is constant for any given high-explosive charge, the triple point growth angle is determined by $k(z)$ and the incident angle. As shown in Figure 1, the convergent detonation wave propagation originates from an annular initiation point O′. As detonation continues, Mach reflection occurs when the incident angle reaches the critical angle. The incident angle is discretized according to the configuration in Figure 1. The value of grid point (n, n) can be obtained from the grid point (n-1, n-1), as shown in Figure 7. The Mach stem height at point (n, n) can be defined as follows:

$$\begin{cases} H_{\mathrm{n}} = \dfrac{R_w \cdot \tan\chi_{n-1} \cdot \tan\varphi_{n-1} - L_{n-1} \cdot \tan\varphi_{n-1} + H_{n-1}}{1 + \tan\chi_{n-1} \cdot \tan\varphi_{n-1}} \\ L_n = \dfrac{L_{n-1} \cdot \tan\chi_{n-1} \cdot \tan\varphi_{n-1} + \tan\varphi_{n-1} \cdot (R_w - H_{n-1})}{1 + \tan\chi_{n-1} \cdot \tan\varphi_{n-1}} \end{cases} \tag{15}$$

where R_w is the radius of the wave-shaper, H_n and L_n are the height and propagation distance of the Mach stem (n = 1, 2, 3…), respectively. The initial conditions in Equation 15 are that when n = 1, $L_1 = R_w \cdot \tan\varphi_0$. By using the data in Table 1 and Equations 9-15, the Mach stem height can be determined.

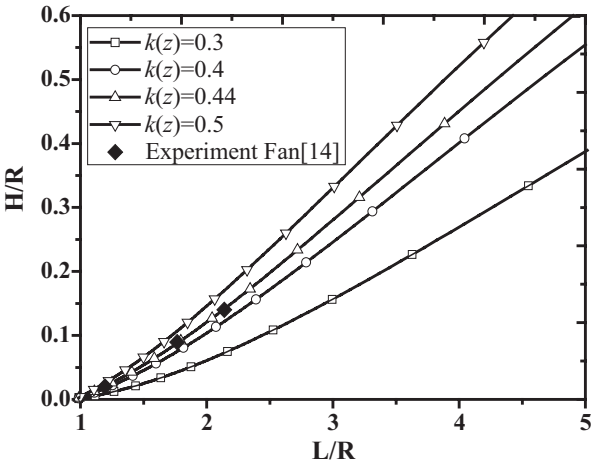

Figure 8. Comparison of the Mach stem height versus the incident angle using different $k(z)$ values.

The analytical model for predicting the Mach stem height was described in the previous section. The input parameters of the analytical model are listed in Table 1, with the exception of $k(z)$ which is a constant determined from the parameters of the high-explosive. A cylindrical high-explosive charge (Table 4) with a wave-shaper is used to measure the Mach stem height. Based on the theoretical calculations, the critical angle of the Mach reflection is 44.7°, which is very close to Fan's experimental results [14]. The existing experimental results [14] and the current analytical model results are compared in Figure 8. With $k(z)$ =0.44, the present model produces Mach stem height results that agree very well with the experimental results.

3 Shock Indentation Experiments on a Cylindrical High-explosive Charge with a Wave-shaper

3.1 Parameters and layout of the shock indentation experiment

The analytical models of detonation wave propagation in a cylindrical high-explosive charge with regular and Mach reflection were presented in Section 2. The impact shock indentation experiment is a method that allows detonation waves or shock waves to collide on a polished metal target and then uses the diameter and depth of the indentation on the surface to obtain the reflection results. Unlike other methods, such as X-ray or high-speed photography [14, 17], the shock indentation experiment is a cost-effective method for directly presenting the interaction results of detonation waves [5, 13, 26]. To obtain the indentation results, a perfectly plastic copper material, called oxygen-free high-conductivity copper, was used as the target in the present study. In order to avoid side face cracks and to reduce the experimental deviation, the dimensions of the target were chosen to be larger than the dimensions of the main charge (D = 50 mm). According to relevant shock indentation experiments [13], the final diameter and thickness of the target were 100 mm and 50 mm, respectively.

The shock indentation experiments are shown schematically in Figure 9. A cylindrical high-explosive charge of the RDX-based explosive (listed in Table 4) was used in the experiments. To obtain an annular initiation detonation wave, a cylindrical nylon piece with a diameter d of 40 mm and length of 30 mm was used as the wave-shaper between the main charge and the para-charge.

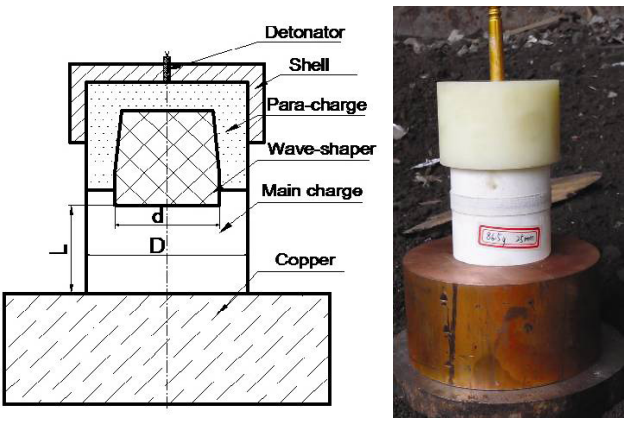

a b

Figure 9. Layout of the cylindrical high-explosive charge with wave-shaper: (a) cross section and (b)image of the experiment before detonation.

As shown in Figure 9a, the cylindrical high-explosive charge under investigation consisted of a wave-shaper, a copper target, a para-charge and a main charge. The diameter and length of the main charge are listed in Table 3. Experiment No. 1 is a comparative experiment, for comparison with other high-explosive charges with a wave-shaper, there being no wave-shaper in experiment No. 1. The parameters of the high-explosive in the main charge and the para-charge are shown in Table 4. To determine the Mach reflection with different incident angles, indentation tests were conducted using five other different lengths of the main charge.

Table 3. Diameter and length of the main charges

No.	L [mm]	Charge mass [g]	Incident angle [°]
1	45	152.5	0.0
2	15	53.5	36.9
3	21	73.4	46.4
4	25	86.6	51.3
5	30	103.1	56.3
6	45	152.5	66.0

Table 4. Parameters of the high-explosive in the main charge and the para-charge.

High Explosive	ρ_0 [g·cm^{-3}]	D_{CJ} [m·s^{-1}]	P_{CJ} [GPa]	E_{CJ} [MPa · m^{3}kg^{-1}]
RDX	1.70	8212	29.6	7.02

3.2 Results

Six experiments were conducted to compare the indentation results of a spherical detonation wave, as well as regular and Mach reflection. A cylindrical high-explosive charge of 50 mm in diameter and 45 mm in length without a wave-shaper was used to generate a traditional spherical detonation wave and its indentation result is shown in Figure 10a. Figure 10b shows a typical indentation result for regular reflection using a main charge length of 15 mm. Here, the incident angle, $\varphi_I = 36.9°$, is smaller than the critical Mach reflection angle $\varphi_{IC} = 44.7°$. A typical indentation result with Mach reflection is shown in Figure 10c with $\varphi_I = 66 > \varphi_{IC}$.

a b c

Figure 10. Indentation results on the surface with different detonation waves: (a) spherical detonation without wave-shaper, (b) regular reflection with wave-shaper, and (c) Mach reflection with wave-shaper.

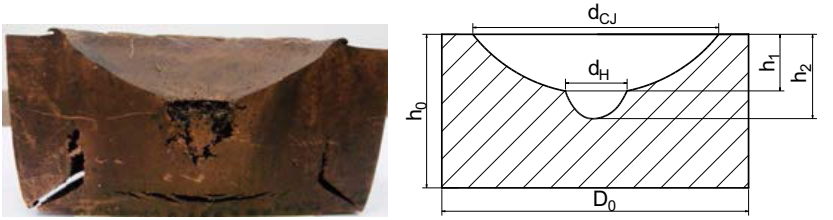

a b

Figure 11. A typical cross sectional configuration after experiment: (a) experimental result, and (b) geometric parameters.

The results show that the copper target has severe plastic deformation where a concave shape is formed as a result of explosive loading. Local cracks and core fractures were formed by the combined effects of the incident shock wave and the reflective wave on the target, as shown in Figure 11a. In addition, a non-perforated hole can be observed in the centre of the target, which was produced by the very high compressive pressure along the axis of the high-explosive charge. The shock indentation experiment with Mach reflection has the largest diameter hole, followed by the one with the regular reflection, and then that with the spherical detonation wave.

The indentation results are listed in Table 5, and the associated parameters are defined in Figure 11b. The increase in the hole diameter is relative to the hole caused by the spherical detonation wave. Also, the regular reflection can be concluded to be caused by the increase in incident pressure. The Mach stem is the main reason for the increase in the hole diameter between the regular and Mach reflection. The Mach stem in shock indentation experiments can be determined

by differentiating the diameter of the hole in the target. Figure 12 shows the indentation results with different incident angles of the Mach reflection. The results show that, as the detonation away from the axis of the charge is close to the Chapman-Jouguet detonation, the values of d_{CJ} are the same on the surface of the copper target. The depth h_2 is greater than the depth h_1 of the normal detonation indentation. The Mach stem height increases with the incident angle of the Mach reflection.

Table 5. Results of the shock indentation experiments*

No.	h_0 [mm]	h_1 [mm]	h_2 [mm]	D_0 [mm]	d_{CJ} [mm]	d_H [mm]
1	51	16.0	25	104	74	8.0
2	51	15.0	22	104	74	16.0
3	52	15.5	24	105	74	16.4
4	52	15.0	22	107	74	17.2
5	52	15.0	21	107	74	18.4
6	56	15.0	20	112	75	21.5

* Parameters defined in Figure 11b.

3.3 Analysis and discussion

The experimental results and theoretical calculations described above are further discussed here. With the propagation of the detonation waves, the characteristics of the Mach stem height in a cylindrical high-explosive charge change with the wave-shaper. A comparison between the theoretical calculations and experimental results of the normalized Mach stem in cylindrical high-explosive charges with a wave-shaper is listed in Table 6, where L is the length of the main charge and R is the radius of the wave-shaper. The results show that, except for experiment No. 3, the deviation of the experimental results and the theoretical calculations were in the range 8.7-13.6%. Due to local cracks being formed on the back of the copper target (Figure 11a), there are some deviations in the experimental data. The calculated and experimental results of the normalized Mach stem in cylindrical high-explosive charges with a wave-shaper are shown in Figure 12. The experimental results are taken from Fan *et al*. [14], who measured the Mach stem heights corresponding to the various lengths of the main charge by using a high-speed camera. With $k(z) = 0.44$, the calculated Mach stem height against the propagation distance agrees well with our experimental data.

Table 6. Comparison between theoretical calculations and experimental results of Mach reflection

No.	Incident angle φ_I [°]	L/R	The normalized Mach stem height		
			Theoretical calculations	Experimental results	Deviation [%]
3	46.40	1.05	0.0085	0.0100	17.6
4	51.30	1.25	0.0267	0.0300	12.4
5	56.30	1.50	0.0552	0.0600	8.7
6	66.04	2.25	0.1592	0.1375	13.6

The results show that when the incident angle is close to the critical angle, the Mach stem height is zero. For incident angles larger than the critical value, the Mach stem height increases as the incident angle increases. However, the pressure and velocity of the Mach stem decrease rapidly and ultimately change to a diverging spherical detonation wave. Although the theoretical calculations show that the Mach stem height increases, the Mach reflection is generally believed to vanish and turn into a Chapman-Jouguet detonation when the parameters of the Mach stem are reduced to the Chapman-Jouguet values.

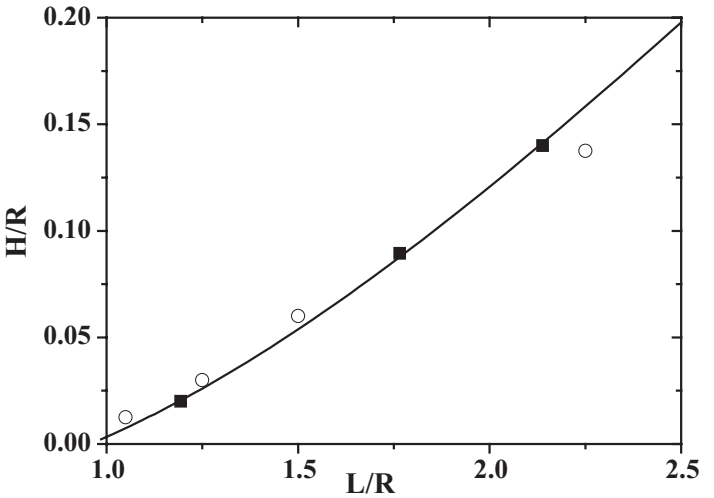

Figure 12. Calculated Mach stem heights and experimental data versus explosive charge length: —, current analytical prediction; ■, experimental results of Fan *et al*. [14], and ○, present experimental results.

4 Conclusions

An analysis of flow fields corresponding to regular and Mach reflection of detonation waves in cylindrical high-explosive charges with a wave-shaper has been undertaken in the current study. Detonation wave propagation in a cylindrical high-explosive charge with a wave-shaper was discussed further. The transition from regular reflection to Mach reflection when the detonation waves interact with each other along the axis of the charge, has been discussed and analyzed. The deflection angle and the critical reflection angle were formulated. The pressure, density and flow velocity of Mach reflection were calculated at the triple and collision points. The triple point growth angle and the intensity of the detonation wave have also been calculated.

The modified Whitham method was used to determine the Mach stem heights. When Mach reflection occurred, with the propagation of the detonation wave, the detonation velocity and pressure of the Mach stem decreased continuously, and the triple point growth angle varied constantly. The results show that the Mach stem height on an RDX-based explosive charge is equal to zero at the critical angle and increases continuously. The Mach stem height based on the present study is about 0.283R when the length L reaches 3R. The corresponding shock indentation experiments on the surface of the copper targets were conducted using a cylindrical high-explosive charge with a wave-shaper. The results showed that the deviation of experimental results and theoretical calculations is in the range 8.7-13.6%, thus proving the validity of the proposed theoretical model.

Acknowledgements

This research was sponsored by the National Program for Support of Top-notch Young Professionals of China. The authors would also like to thank the State Key Laboratory of Explosion Science and Technology (Beijing Institute of Technology) (KFJJ15-07M) for their great support of the research work presented in this paper.

References

[1] Dowker J.S., Quantum Mechanics on Group Space and Huygens' Principle, *Ann. Phys. (Amsterdam, Neth.)*, **1971**, *62*(2), 361-382.

[2] Zhu C.S., Huang Z.X., Zu X.D., Xiao Q.Q., Mach Wave Control in Explosively Formed Projectile Warhead, *Propellants Explos. Pyrotech*., **2014**, *39*(6), 909-915.

[3] Zhang Y.G., Zhang X.F., He Y., Qiao L., Detonation Wave Propagation in Shaped

Charges with Large Wave-shaper, *27th Int. Symp. Ballistics*, Freiberg, Germany, **2013**, 770-782.
[4] Al'tshule L.V.R, Zubarev V.N., Telegin G.S., Supercompressed Detonation Waves in Condensed Explosives, *Combust. Explos. Shock Waves (Engl. Transl.)*, **1974**, *10*(5), 648-652.
[5] Dunne B.B., Mach Reflection of Detonation Waves in Condensed High Explosive, *Phys. Fluids*, **1961**, *4*(7), 918-933.
[6] Dunne B.B., Mach Reflection of Detonation Waves in Condensed High Explosive II, *Phys. Fluids*, **1964**, *7*(10), 1707-1712.
[7] Krishnan S., Brochet C., Cheret R., Mach Reflection in Condensed Explosives, *Propellants Explos. Pyrotech.*, **1981**, *6*(6), 170-172.
[8] Trotsyuk A.V., Kudryavtsev A.N., Ivanov M.S., Mach Reflection of Shock and Detonation Waves in Steady Supersonic Chemically Reacting Flows, *Proc. Int. Conf. on Recent Advances in Space Technologies*, Istanbul, Turkey, **2003**, 495-503.
[9] Wang L., Mach Stem Height in Pseudo-steady and Unsteady Mach Reflection, *Journal of Fudan University (Natural Science)*, **2010**, *49*(4), 513-519.
[10] Hull L.M., *Mach Reflection of Spherical Detonation Waves*, Report No. LA-UR-93-2080, **1993**.
[11] Hull L.M., *Detonation Propagation and Mach Stem Formation in PBXN-9*, Report No. LA-UR-97-3827, **1997**.
[12] Zhang X.F., Huang Z.X., Qiao L., Detonation Wave Propagation in Double-layer Cylindrical High Explosive Charge, *Propellants Explos. Pyrotech.*, **2011**, *36*(3), 210-218.
[13] Cao B., Yu Z.Y., Chen H.W., An Experimental Investigation on the Loading Performance and Propagation Law of Detonation Mach-waves (in Chinese), *Journal of Ballistics*, **2000**, *12*(2), 79-83.
[14] Fan B.C., Yang Q.Z., Yang S.H., The Propagation and Interactions of Axisymmetric Detonation Waves (in Chinese), *Explosive and Shock Waves*, **1984**, *4*(1), 68-77.
[15] Grasso F., Paoli R., An Analytical Study of Mach Reflection in Nonequilibrium Steady Flows, *Phys. Fluids*, **1999**, *11*(10), 3150-3167.
[16] Chpoun A., Passerel D., Li H., Ben-Dor G., Reconsideration of Oblique Shock Wave Reflections in Steady Flows, Part 1. Experimental Investigation, *J. Fluid Mech.*, **1995**, *301*, 19-35.
[17] Teng H.H., Jiang Z.L., Gasdynamic Characteristics of Toroidal Shock and Detonation Wave Converging, *Science in China Series G: Physics and Astronomy*, **2005**, *48*(6), 739-749.
[18] Panov K.N., Konmrachkov V.A., Tselikov I.S., Radiographic Study of Interaction of Shock and Detonation Waves in a High Explosive, *Combust., Explos. Shock Waves (Engl. Transl.)*, **2007**, *43*(3), 365-371.
[19] Levin V.A., Manuylovich I.S., Markov V.V., Detonation in Supersonic Flows in Channels with Obstacles, *28th Int. Symp. on Shock Waves*, Heidelberg, Germany, **2012**, 397-402.
[20] Li J., Ning J., Lee J.H.S., Mach Reflection of a ZND Detonation Wave, *Shock*

Waves, **2015**, *25*(3), 293-304.
[21] Sternberg H.M., Piacesi D., Interaction of Oblique Detonation Waves with Iron, *Phys. Fluids*, **1966**, *9*(7), 1307-1315.
[22] Whitham G.B., A New Approach to Problems of Shock Dynamics. Part I. Two-dimension Problem, *J. Fluid Mech.*, **1957**, *2*(02), 145-171.
[23] Whitham G.B., *Linear and Nonlinear Waves*, Vol. 8, Shock Dynamics, John Wiley & Sons, New York – London – Sydney – Toronto, **1974**, pp. 263-311; ISBN 0-471-94090-9.
[24] Lambourn B.D., Wright P.W., Mach Interaction of Two Plane Detonation Waves, *Proc.4th Symp. on Detonation*, Office of Naval Research Arlington, VA, USA, **1965**, 142-152.
[25] Zhang J.X., Yun S.R., Experimental Investigations of the Mach Reflection in a Condensed Explosive (in Chinese), *Explosive and Shock Waves*, **1986**, *6*(3), 208-213.
[26] Müller F., Mach-reflection of Detonation Waves in Condensed High Explosives, *Propellants Explos. Pyrotech.*, **1978**, *3*(4), 115-118.